4440 *Inorg. Chem.* **2010**, *49*, 4440–4446
DOI: 10.1021/ic9022085

Inorganic Chemistry
Article

New Chiral and Flexible Metal−Organic Framework with a Bifunctional Spiro Linker and Zn_4O-Nodes

Kristina Gedrich,[†] Irena Senkovska,[†] Igor A. Baburin,[‡] Uwe Mueller,[§] Oliver Trapp,[∥] and Stefan Kaskel*[,†]

[†]*Department of Inorganic Chemistry, Dresden University of Technology, Mommsenstrasse 6, D-01069 Dresden, Germany,* [‡]*Max Planck Institute for Chemical Physics of Solids, Nöthnitzer Strasse 40, D-01187 Dresden, Germany,* [§]*Helmholtz-Zentrum Berlin für Materialien und Energie, Institute Soft Matter and Functional Materials, BESSY-MX Group, Albert-Einstein-Strasse 15, D-12489 Berlin, Germany, and* [∥]*Organisch-Chemisches Institut, Ruprecht-Karls-Universität Heidelberg, Im Neuenheimer Feld 270, D-69120 Heidelberg, Germany*

Received November 9, 2009

A new chiral Metal−Organic Framework (MOF), named DUT-7, has been synthesized from enantiopure (*S*)-2,2′-spirobiindane-5,5′-dicarboxylic acid ((*S*)-H_2L) and zinc nitrate. The framework of the compound has the composition Zn_4O((*S*)-L)$_3$ as it is found for the IRMOF series, but in contrast to these MOFs, the crystal structure of DUT-7(RT) (RT: room temperature) which has to be assigned to the chiral space group $P6_322$, has a completely different topology. The Zn_4O clusters are not coordinated in an octahedral fashion but show only C_3 symmetry and are arranged in a trigonal-prismatic manner. The framework is built of two interpenetrated nets with an **acs** topology related to each other by the 2-fold axes. DUT-7 is the first example of this rare framework topology constructed from Zn_4O units. A reversible structural transformation was observed upon cooling during single crystal X-ray diffraction. The resulting crystal structure, denoted as DUT-7(LT) (LT: low temperature), is characterized by a Zn_4O cluster not only coordinated by six linker moieties but also by two additional solvent molecules leading to an octahedral coordination of one of the zinc atoms of the cluster. This structure transformation leads to a tripled unit cell compared to DUT-7(RT) and a change of the space group to $P6_522$. The flexibility of the coordination of the metal atoms which has been observed for the first time points toward a catalytic activity of MOFs exhibiting metal atoms with a closed shell not only caused by defects in the crystal structure. The reaction of racemic 2,2′-spirobiindane-5,5′-dicarboxylic acid (*rac*-H_2L) with zinc nitrate lead to a microcrystalline compound DUT-7(*rac*). DUT-7 and DUT-7(*rac*) have been characterized by X-ray powder diffraction, elemental and thermogravimetric analysis, and IR spectroscopy revealing the same framework composition for both compounds. The porosity of DUT-7 and DUT-7(*rac*) was proven by nitrogen and hydrogen physisorption measurements.

Introduction

Metal−Organic Frameworks (MOFs), a new class of highly porous materials,[1−3] have attracted a lot of interest since the early synthesis and characterization of the highly stable and porous materials such as MOF-5 by Yaghi and co-workers in 1999.[4] Pertaining to the class of hybrid organic inorganic materials, MOFs are built of metal atoms or metal clusters, so-called nodes, linked by multifunctional carboxylates or N-donor ligands. This assembly leads to materials exhibiting high crystallinity combined with extraordinary large specific surface areas and pore volumes exceeding those of established porous materials such as zeolites or active carbons. Numerous new MOFs have been synthesized and characterized up to now with different objectives. On the one hand there is a need for materials with high storage capacities for methane or hydrogen enabling the application of natural gas or hydrogen as fuel for motorized vehicles.[5,6] On the other hand, the use of MOFs for separation or purification processes is extensively studied.[7,8] A third field of application

*To whom correspondence should be addressed. E-mail: stefan.kaskel@chemie.tu-dresden.de. Fax: (+49)0351-46337287.

(1) Kitagawa, S.; Kitaura, R.; Noro, S.-i. *Angew. Chem., Int. Ed.* **2004**, *43*, 2334–2375.
(2) Férey, G. *Stud. Surf. Sci. Catal.* **2007**, *170A*, 66–86.
(3) Kaskel, S. Porous Metal-Organic Frameworks. In *Handbook of Porous Solids*; Schüth, F., Sing, K. S. W., Weitkamp, J., Eds.; Wiley-VCH: Weinheim, Germany, 2002; Vol. *2*, pp 1190−1249.
(4) Li, H.; Eddaoudi, M.; O'Keeffe, M.; Yaghi, M. *Nature* **1999**, *402*, 276–279.
(5) Murray, L. J.; Dinca, M.; Long, J. R. *Chem. Soc. Rev.* **2009**, *38*, 1294–1314.
(6) Senkovska, I.; Kaskel, S. *Microporous Mesoporous Mater.* **2008**, *112*, 108–115.
(7) Li, J.-R.; Kuppler, R. J.; Zhou, H.-C. *Chem. Soc. Rev.* **2009**, *38*, 1477–1504.
(8) Alaerts, L.; Kirshhock, C. E. A.; Maes, M.; van der Veen, M. A.; Finsy, V.; Depla, A.; Martens, J. A.; Baron, G. V.; Jacobs, P. A.; Denayer, J. F. M.; De Vos, D. E. *Angew. Chem., Int. Ed.* **2007**, *46*, 4293–4297.

 Published on Web 04/15/2010

is the use of MOFs as catalysts themselves or as catalyst supports.[9−11] In this context, the use of chiral linkers for the development of new catalysts combining heterogeneity with the activity and stereoselectivity achieved with homogeneous catalysts has to be mentioned.[12,13] The first example was published by Kim et al. using a chiral linker derived from tartaric acid to obtain a homochiral, catalytically active and enantioselective MOF called POST-1.[14] Since then, different chiral MOFs have been synthesized using different approaches. The group of Lin has studied extensively the application of axial chiral binaphthyl linkers.[13,15−17] Especially, the use of orthogonally functionalized binaphthyl linkers exhibiting secondary functional groups for the incorporation of catalytically active metal centers has been shown to be extremely successful. Besides that, different groups successfully integrated molecules from the chiral pool into MOFs.[18−20] Even the homogeneous Jacobsens catalyst for the enantioselective epoxidation of olefins could be immobilized by the incorporation of functional groups and their fixation in a framework.[21] Furthermore, chiral 4,4′-bipyridyls[22] and bis-triazoles[23] could be incorporated into MOF structures.

The mentioned examples show that especially readily available chiral molecules or chiral ligands established in homogeneous stereoselective catalysis can be used for the construction of chiral MOF catalysts. A group not yet considered is the ligand class with a chiral spiro backbone though they have been shown to be extremely successful in homogeneous catalysis.[24−26] Because of the tetrahedral coordination of the quarternary spiro carbon atom and the perpendicular arrangement of the two rings linked by it, these ligands are extremely rigid and a racemization is virtually excluded. These characteristics make molecules containing a spiro backbone ideally suited for the construction of chiral MOFs.

Up to date, only few examples of coordination polymers built of spiro linkers have been published. The first one, reported by Wong et al. in 2005, describes the formation of one-dimensional strands using a chiral linker with a 9,9′-spirobifluorene backbone and silver atoms.[27] Since the racemic mixture of the linker was used the resulting coordination polymer contains both enantiomeric forms. In two further publications symmetrically 4-fold substituted and thus nonchiral 9,9′-spirobifluorenes were used for the construction of coordination polymers. If the spirobifluorene backbone is functionalized by carboxylate groups, only a two-dimensional layered structure containing cobalt could be obtained.[28] Zhou and co-workers applied a 4-fold tetrazolate substituted spirobifluorene, and they were the first succeeding in the formation of three-dimensional framework structures.[29] Unfortunately, these non chiral materials exhibit no permanent porosity upon solvent removal.

Chart 1. Structure of (*R*)- and (*S*)-2,2′-Spirobiindane-5,5′-dicarboxylic Acid

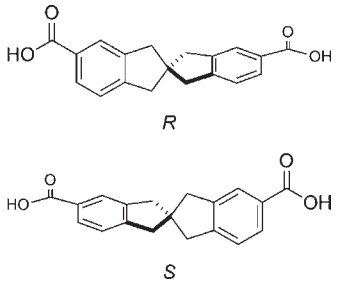

In the following, we present the synthesis and characterization of the first chiral, three-dimensional porous framework built of a linker with a 2,2′-spirobiindane backbone, named DUT-7 (DUT: Dresden University of Technology). Our efforts aimed at the synthesis of the chiral linker 2,2′-spirobiindane-5,5′-dicarboxylic acid (H_2L, Chart 1) starting from diethylmalonate and benzyl chloride according to procedures described by Maslak et al.[30] and Neudeck and Schlögl.[31]

Experimental Section

General Remarks. Zinc nitrate tetrahydrate (≥98.5%, Merck) was used as received. *N*,*N*-Dimethylformamide (DMF) was dried over phosphorus pentoxide and stored under argon atmosphere.

Powder X-ray diffraction (PXRD) patterns were obtained in transmission geometry using a Stoe StadiP X-ray diffractometer equipped with an IPDS detector and monochromated Cu−Kα1 (λ = 0.15405 nm) radiation (40 kV, 30 mA) with a scan speed of 30 s/step and a step size of 0.1°. Gas physisorption measurements were performed at 77 K using a Quantachrome AUTOSORB 1C apparatus. Thermogravimetric analyses (TG) were carried out under air atmosphere using a Netzsch STA 409 thermal analyzer. Infrared spectra (IR) were recorded in diffuse reflection geometry using a BIORAD Excalibur FTS3000 (Varian Inc.) infrared spectrometer. Elemental analysis (C, H, N) was performed with a CHNS 932 analyzer from LECO. The oxygen content was determined by coupling of the CHNS 932 analyzer with the pyrolysis furnace VTF-900. The zinc

(9) Lee, J. Y.; Farha, O. K.; Roberts, J.; Scheidt, K. A.; Nguyen, S. B. T.; Hupp, J. T. *Chem. Soc. Rev.* **2009**, *38*, 1450–1459.
(10) Farrusseng, D.; Aguado, S.; Pinel, C. *Angew. Chem., Int. Ed.* **2009**, *48*, 7502–7513.
(11) Czaja, A. U.; Trukhan, N.; Muller, U. *Chem. Soc. Rev.* **2009**, *38*, 1284–1293.
(12) Ma, L.; Abney, C.; Lin, W. *Chem. Soc. Rev.* **2009**, *38*, 1248–1256.
(13) Lin, W. *J. Solid State Chem.* **2005**, *178*, 2486–2490.
(14) Seo, J. S.; Whang, D.; Lee, H.; Jun, S. I.; Oh, J.; Jeon, Y. J.; Kim, K. *Nature* **2000**, *404*, 982–986.
(15) Evans, O. R.; Ngo, H. L.; Lin, W. *J. Am. Chem. Soc.* **2001**, *123*, 10395–10396.
(16) Wu, C.-D.; Hu, A.; Zhang, L.; Lin, W. *J. Am. Chem. Soc.* **2005**, *127*, 8940–8941.
(17) Ma, L.; Lin, W. *J. Am. Chem. Soc.* **2008**, *130*, 13834–13835.
(18) Vaidhyanathan, R.; Bradshaw, D.; Rebilly, J.-N.; Barrio, J. P.; Gould, J. A.; Berry, N. G.; Rosseinsky, M. J. *Angew. Chem., Int. Ed.* **2006**, *45*, 6495–6499.
(19) Dybtsev, D. N.; Nuzhdin, A. L.; Chun, H.; Bryliakov, K. P.; Talsi, E. P.; Fedin, V. P.; Kim, K. *Angew. Chem., Int. Ed.* **2006**, *45*, 916–920.
(20) Zeng, M.-H.; Wang, B.; Wang, X.-Y.; Zhang, W.-X.; Chen, X.-M.; Gao, S. *Inorg. Chem.* **2006**, *45*, 7069–7076.
(21) Cho, S.-H.; Ma, B.; Nguyen, S. T.; Hupp, J. T.; Albrecht-Schmitt, T. E. *Chem. Commun.* **2006**, 2563–2565.
(22) Sbircea, L.; Sharma, N. D.; Clegg, W.; Harrington, R. W.; Horton, P. N.; Hursthouse, M. B.; Apperley, D. C.; Boyd, D. R.; James, S. L. *Chem. Commun.* **2008**, 5538–5540.
(23) Iremonger, S. S.; Southon, P. D.; Kepert, C. J. *Dalton Trans.* **2008**, 6103–6105.
(24) Ding, K.; Han, Z.; Wang, Z. *Chem. Asian J.* **2009**, *4*, 32–41.
(25) Xie, J.-H.; Zhou, Q.-L. *Acc. Chem. Res.* **2008**, *41*, 581–593.
(26) Xie, J.-H.; Zhu, S.-F.; Fu, Y.; Hu, A.-G.; Zhou, Q.-L. *Pure Appl. Chem.* **2005**, *77*, 2121–2132.
(27) Wong, K.-T.; Liao, Y.-L.; Peng, Y.-C.; Wang, C.-C.; Lin, S.-Y.; Yang, C.-H.; Tseng, S.-M.; Lee, G.-H.; Peng, S.-M. *Cryst. Growth Des.* **2005**, *5*, 667–671.
(28) Clews, P. K.; Douthwaite, R. E.; Kariuki, B. M.; Moore, T.; Taboada, M. *Cryst. Growth Des.* **2006**, *6*, 1991–1994.
(29) Collins, C. S.; Sun, D.; Liu, W.; Zuo, J.-L.; Zhou, H.-C. *J. Mol. Struct.* **2008**, *890*, 163–169.
(30) Maslak, P.; Varadarajan, S.; Burkey, J. D. *J. Org. Chem.* **1999**, *64*, 8201–8209.
(31) Neudeck, H.; Schlögl, K. *Chem. Ber.* **1977**, *110*, 2624–2639.

Table 1. Crystal Data and Structure Refinement Information for DUT-7(RT) and DUT-7(LT)

	DUT-7(RT)	DUT-7(LT)
empirical formula	$C_{57}H_{42}O_{13}Zn_4$	$C_{63}H_{56}N_2O_{15}Zn_4$
formula weight	1196.39	1342.58
temperature	263(2) K	100(2) K
radiation, wavelength	synchrotron, 0.88561 Å	synchrotron, 0.88561 Å
crystal system	hexagonal	hexagonal
space group	$P6_322$ (No. 182)	$P6_522$ (No. 179)
unit cell dimensions	a = 22.249(3) Å c = 25.906(5) Å	a = 21.560(3) Å c = 77.814(16) Å
volume	11106(3) Å^3	31325(9) Å^3
Z	4	12
density (calculated)	0.716 g cm^{-3}	0.854 g cm^{-3}
F(000)	2432	8256
crystal size	0.4 × 0.3 × 0.2 mm^3	0.4 × 0.3 × 0.2 mm^3
θ range for data collection	2.28 to 30.59°	1.36 to 36.23°
index ranges	$-12 \le h \le 12$ $-25 \le k \le 25$ $-29 \le l \le 29$	$-26 \le h \le 26$ $-27 \le k \le 22$ $-79 \le l \le 93$
reflections collected	30068	109171
independent reflections	5830 [R(int) = 0.0437]	23119 [R(int) = 0.1059]
completeness to θ	98.8%	90.5%
refinement method	full-matrix least-squares on F^2	full-matrix least-squares on F^2
data/restraints/parameters	5830/0/225	23119/496/726
goodness-of-fit on F^2	1.021	0.900
final R indices [$I > 2\sigma(I)$]	R_1 = 0.0467, wR_2 = 0.1321	R_1 = 0.0551, wR_2 = 0.1308
R indices (all data)	R_1 = 0.0509, wR_2 = 0.1360	R_1 = 0.0958, wR_2 = 0.1443
absolute structure parameter	−0.025(18)	−0.080(11)
largest diff. peak and hole	0.616 and −0.270 e Å^{-3}	0.448 and −0.680 e Å^{-3}

content was determined with an ICP-OES Vista RL apparatus from Varian Inc.

Synthesis of 2,2′-Spirobiindane-5,5′-dicarboxylic Acid. 2,2′-Spirobiindane-5,5′-dicarboxylic acid was synthesized according to literature procedures.[30,31] The resulting racemic mixture of H_2L was separated by enantioselective preparative HPLC using a Shimadzu LC-8A equipped with a Sepapak 1 column (20 μm, 196 × 48 mm) and the fraction collector FRC-10A. Iso-hexane/2-propanol/trifluoroacetic acid (90:10:0.2 v/v/v) was used as the mobile phase. The pressure was 2.8 MPa and the temperature 308 K. ^{1}H NMR (500 MHz, DMSO-d6); δ(ppm): 2.96 (s, 4 H, 1-H, 1′-H or 3-H, 3′-H), 2.97 (s, 4 H, 3-H, 3′-H or 1-H, 1′-H), 7.32 (d, $^3J_{HH}$ = 7.9 Hz, 2 H, 7-H, 7′-H), 7.75 (d, $^3J_{HH}$ = 7.9 Hz, 2 H, 6-H, 6′-H), 7.78 (s, 2 H, 4-H, 4′-H), 12.74 (s, 2 H, COOH). ^{13}C NMR (500 MHz, DMSO-d6); δ (ppm): 44.52, 44.81, 52.63, 124.63, 125.52, 127.89, 129.10, 143.30, 148.35, 167.58. Elemental analysis: wt % obs. (calc.): C: 73.63 (74.01), H: 5.91 (5.23). IR (cm^{-1}): 413 (m), 554 (m), 646 (m), 763 (s), 839 (m), 934 (s), 1043 (w), 1093 (m, 1124 (m), 1176 (m), 1214 (m), 1306 (s), 1335 (w), 1440 (s), 1492 (m), 1579 (s), 1614 (s), 1698 (s), 1916 (w), 2039 (w), 2190 (w), 2555 (w), 2598 (w), 2667 (w), 2843 (w), 2903 (w), 2941 (w), 2400−3300 (br).

Synthesis of $Zn_4O((S)\text{-}L)_3(DMF)_{10}(H_2O)_{3.5}$ (DUT-7) and $Zn_4O(rac\text{-}L)_3(DMF)_4(H_2O)_{2.3}$ (DUT-7(*rac*)). An 86 mg portion of (*S*)-H_2L or *rac*-H_2L (0.28 mmol), respectively, and 110 mg of $Zn(NO_3)_2 \cdot 4\,H_2O$ (0.42 mmol) were dissolved in 14 mL of DMF. The solution was heated in a Pyrex tube at 393 K for 20 h. The resulting colorless crystals of DUT-7 or the off-white, microcrystalline solid DUT-7(*rac*) were collected by filtration under argon, washed twice with DMF, and dried in an argon flow at room temperature. For DUT-7: Yield: 146 mg (79%, referred to the amount of (*S*)-H_2L). Elemental analysis: wt % obs. ± σ (calc.): C: 52.8 ± 0.4 (52.5), H: 6.06 ± 0.10 (6.03), N: 6.87 ± 0.07 (7.04), O: 21.6 ± 0.3 (21.3), Zn: 12.7 ± 0.2 (13.1). IR (cm^{-1}): 542 (m), 600 (w), 665 (s), 772 (s), 806 (m), 851 (w), 928 (m), 1090 (s), 1225 (w), 1258 (m), 1329 (w), 1393 (s), 1427 (s), 1495 (m), 1568 (s), 1603 (s), 1651 (s), 1682 (s), 2837 (m), 2891 (w), 2930 (m), 3017 (w), 3061 (m). For DUT-7(*rac*): Yield: 106 mg (74%, referred to the amount of *rac*-H_2L). Elemental analysis: wt % obs. ± σ (calc.): C: 53.9 ± 0.3 (54.2), H: 4.96 ± 0.09 (4.91), N: 3.39 ± 0.09 (3.66), O: 19.9 ± 0.1 (20.2), Zn: 17.58 ± 0.05 (17.09). IR (cm^{-1}): 544 (s), 613 (m), 661 (s), 776 (s), 796 (m), 806 (m), 851 (m), 929 (m), 1101 (s), 1214 (m), 1262 (m), 1393 (m),1417 (s), 1444 (s), 1495 (m), 1573 (s), 1619 (s), 1683 (s), 2837 (m), 2895 (m), 2930 (m), 3019 (m), 3063 (m).

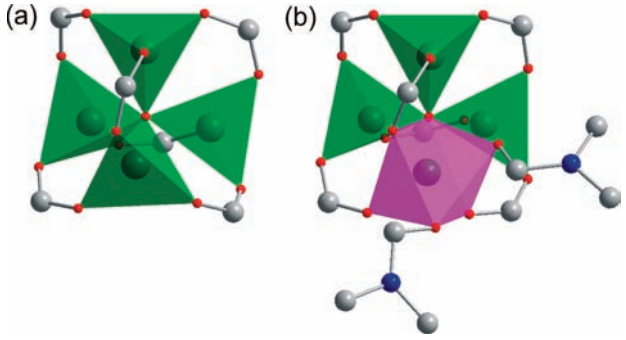

Figure 1. Zn_4O clusters contained (a) in DUT-7(RT) and (b) in DUT-7(LT).

X-ray Crystallography. A crystal of DUT-7 was taken directly from the mother liquor, transferred to Paratone-N oil and mounted into a CryoLoop (both Hampton Research Corp.). The data were collected using synchrotron radiation on beamline BL14.2 of the Joint Berlin-MX Laboratory at BESSY-II (Berlin, Germany) with a MX-225 CCD detector (Rayonics, Illinois) at 263 and 100 K, respectively. The data were integrated and scaled with XDS Software[32] (For further details, see Table 1). The structure of DUT-7(RT) was solved using direct methods, the structure of DUT-7(LT) using Patterson method with the help of SHELXS-97[33] and refined by full-matrix least-squares techniques using SHELXL-97.[34] Non-hydrogen atoms of the networks were refined with anisotropic temperature parameters. The hydrogen atoms were positioned geometrically and refined using a riding model. Because of the high symmetry of the space group and low residual electron density, it was impossible to locate the guest molecules in the crystal structure of DUT-7(RT). For the DMF molecules in DUT-7(LT), the following distance restraints were imposed: O15−N2 and O14−N1 2.23(2), L22-L23 and L12-L13 2.48(2). The molecule was also restrained to be approximately planar, and the atoms were restrained to vibrate in a nearly isotropic manner. Application of the SQUEEZE[35] routine in the PLATON software package produced a new intensity data set excluding the intensity contribution from disordered solvent molecules. CCDC-753236 for DUT-7(RT) and CCDC-753235 for DUT-7(LT) contain the supplementary crystallographic data for this paper. These data can be obtained free of charge from the Cambridge Crystallographic Data Centre via www.ccdc.cam.ac.uk/data_request/cif. The topology of the network has been examined with the program package TOPOS.[36]

(32) Kabsch, W. *J. Appl. Crystallogr.* **1993**, *26*, 795–800.
(33) Sheldrick, G. M. *SHELXS-97*, 97−2; University of Göttingen: Göttingen, Germany: 1997.
(34) Sheldrick, G. M. *SHELXL-97*, 97−2; University of Göttingen: Göttingen, Germany: 1997.
(35) Van der Sluis, P.; Spek, A. L. *Acta Crystallogr., Sect. A* **1990**, *A46*, 194–201.
(36) Blatov, V. A. *IUCr Compcomm Newsletter* **2006**, *7*, 4–38.

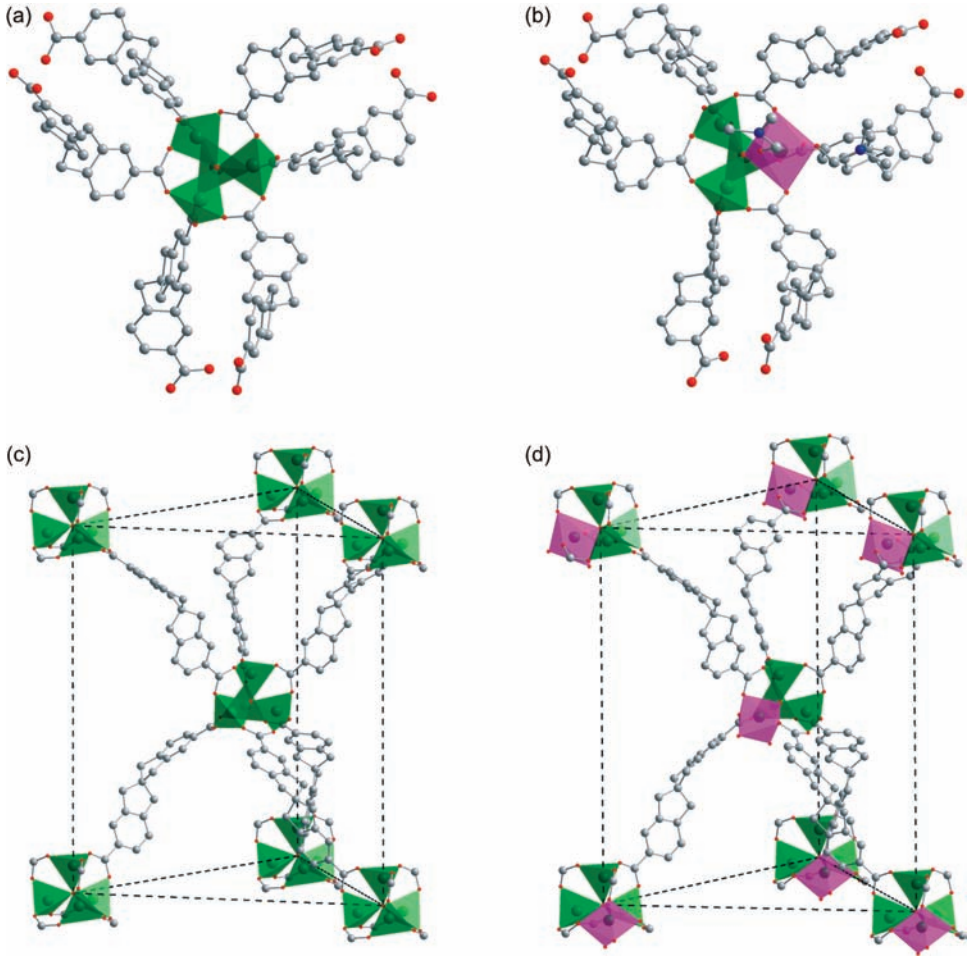

Figure 2. (a) SBUs of DUT-7(RT) and (b) DUT-7(LT), both: view along [001]; (c) Trigonal prismatic coordination of Zn_4O cluster in DUT-7(RT), (d) kept in DUT-7(LT) in spite of the additionally coordinated solvent molecules (DMF molecules were omitted in (d) for clarity).

Results and Discussion

Synthesis and Crystal Structure of Zn_4O((*S*)-L)$_3$ (DUT-7). The reaction of (*S*)-H_2L with an excess of zinc nitrate tetrahydrate in DMF at 393 K led to colorless crystals of DUT-7. The crystal structure of DUT-7 was determined at two different temperatures, 263 and 100 K (see Experimental Section for details). The compound crystallizes in the hexagonal crystal system. While the lattice constant *a* is only slightly changed upon cooling (263 K: a = 22.249 Å, 100 K: a = 21.560 Å) the length of the lattice constant *c* was tripled (263 K: c = 25.906 Å, 100 K: c = 77.814 Å). Owing to this obvious structural change during the cooling procedure the crystal structure determined at 263 K will be denoted as DUT-7(RT) whereas the low temperature structure (100 K) will be denoted as DUT-7(LT) in the following.

Single crystal X-ray analysis revealed that DUT-7(RT) crystallizes in the chiral space group $P6_322$ and DUT-7(LT) in $P6_522$. In the crystal structure of DUT-7(RT) Zn_4O clusters act as nodes (Figure 1) and are interlinked by the spiro linker (*S*)-L to form a three-dimensional network. Lying on a 3-fold axis, the cluster contains only two independent zinc atoms, all of them tetrahedrally coordinated by oxygen atoms. The Zn−O distances range from 1.92(2) to 1.95(9) Å, and the O−Zn−O angles are in the range of 104.7(5) to 112.0(8) °. The carbon atoms of the carboxylate groups are nearly perfectly octahedrally arranged around the central μ_4O-atom since the C−O−C angles range from 88.0(1) to 92.5(1)°. Instead of an octahedral arrangement of the six neighboring Zn_4O clusters around the central one, the Secondary Building Unit (SBU) has C_3 symmetry and is surrounded by six neighboring clusters in a trigonal-prismatic fashion (Figure 2).

In contrast to the structure of DUT-7(RT), the tetrahedral coordination of one zinc atom of the Zn_4O cluster in DUT-7(LT) is changed upon cooling since two molecules from the solvent contained in the pores are coordinated additionally leading to an octahedral coordination of one of the four zinc atoms (Figure 1). The Zn−O distances of the tetrahedrally coordinated zinc atoms range from 1.91(6) to 1.99(8) Å, and the O−Zn−O angles are in the range of 101.1(8)−122.2(1)°. Thus, the nearly ideal tetrahedral coordination of the zinc atoms found in DUT-7(RT) is noticeably distorted during the cooling process. In contrast, the tetrahedral coordination of the μ_4O-atom is not heavily distorted (Zn−O distances: 1.91(6)−2.00(4) Å, Zn−O−Zn angles: 107.2(1)−111.7(3)°). The Zn−O distances of the octahedrally coordinated zinc atom (2.00(4)−2.22(4) Å) are on the whole longer than found for the tetrahedrally coordinated ones. The longest Zn−O distances are observed for the coordinated solvent molecules (2.14(8) Å and 2.22(4) Å). As it was found for the tetrahedrally coordinated zinc atoms, the O−Zn−O angles around the octahedrally coordinated zinc atom (83.5(9)−104.9(8)°) differ significantly from the ideal

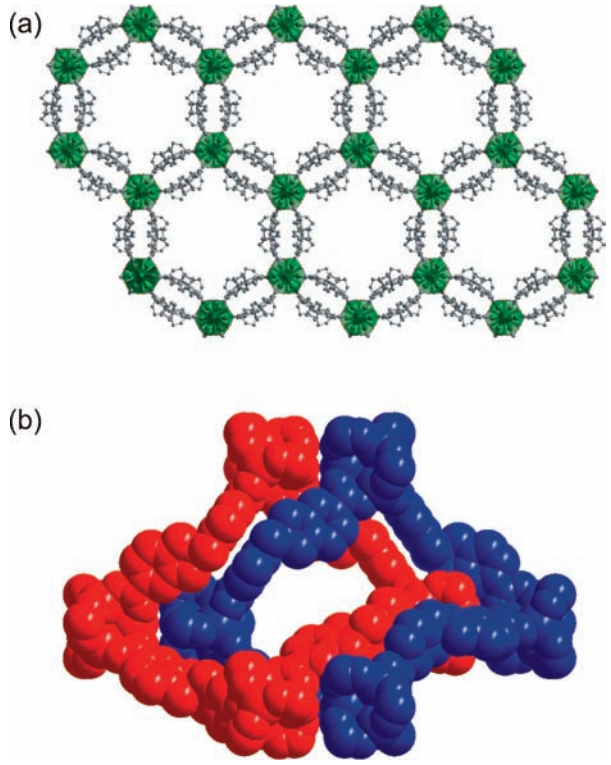

Figure 3. (a) Hexagonal channels within the crystal structure of DUT-7(RT) (view along [001]). (b) Quadrangular pore windows (view along [100]), the interpenetrated nets are shown in red and blue, respectively.

value of 90°. Thus, the former ideal arrangement of the carboxylate groups around the μ_4O-atom is broken up (C−O−C angles: 80.5(1)−110.8(2) °) lowering the symmetry of the SBU to C_1 (Figure 2).

Furthermore, the conformation of the linker is changed during the cooling process indicated by bending/widening of the angle between the carbon atoms of the carboxy groups belonging to one linker and the spiro carbon atom of the same ligand. For the room temperature conformation DUT-7(RT) this angle is found to have a value of 148.8(1)°. In the crystal structure of DUT-7(LT) this angle has values of 139.0(1)°, 144.0(1)°, and 164.9(1)° (DUT-7(LT) contains three symmetrically independent linkers) being significantly different from the one found at 263 K.

The structural transformation described in the foregoing sections is reversible since upon warming of the single crystal to 263 K the smaller unit cell is found again. To the best of our knowledge this is the first example demonstrating the structural flexibility of the Zn_4O nodes in MOFs. Up to now, two MOF structures comprising Zn_4O nodes with additionally coordinated solvent molecules (DMF and dimethylsulfoxide) are known[37,38] but a reversible change of the coordination number of the metal atoms in the cluster has not been reported yet. Since one of the zinc atoms is able to coordinate two additional solvent molecules, the positions occupied by them can be seen as potentially accessible metal sites. This finding points toward a catalytic activity of MOFs containing Zn_4O clusters not only caused by defects in the crystal structure as it is often considered[39] but also by expanded coordination numbers corresponding to transition states with a very short lifetime.

Instead of the formation of a cubic framework, the SBUs in DUT-7(RT) are interconnected in a helical fashion forming hexagonal channels parallel to the *c* axis with a diameter of approximately 19 Å (Figure 3a; all distances are given for atom center to atom center). By the intersection of three adjacent hexagonal channels quadrangular pore windows with a size of approximately 12 × 18 Å are formed (Figure 3b; either the red or the blue net).

The structure of DUT-7(RT) consists of two interpenetrating networks (Figure 4, bottom). The second network does not diminish the diameter of the hexagonal channels but that of the quadrangular pore windows to about 8 × 14 Å (Figure 3b) as it is only "shifted" along the *c* axis compared to the first network. Overall, the void space of the crystal structure of DUT-7(RT) amounts to 63% calculated with PLATON.[40] The interpenetrating networks are attached to each other by $\pi-\pi$ interactions. Both aromatic rings of each 2,2′-spirobiindane-5,5′-dicarboxylate moiety interact with two organic linkers from the second interpenetrating network (Figure 5). The first pair of aromatic rings has an angle of 15.7(4)° leading to distances between 3.51(1) and 4.22(2) Å. The planes containing the second pair of aromatic rings are nearly parallel (enclosed angle: 1.0(5)°). The distance between these rings is in the range of 3.79(2) to 3.94(1) Å.

The PXRD pattern of the as-made material DUT-7 and the calculated patterns for DUT-7(RT) and DUT-7(LT) are presented in Figure 6.

Topological Analysis. The topology of DUT-7 is that of the **acs** net. In its idealized form (space group $P6_3/mmc$, site symmetry D_{3h}[41]) it has trigonal-prismatic coordination of nodes (Figure 4, top) and, therefore, was proposed to be a "default" pattern for linking trigonal-prismatic building blocks.[42,43] However, quite recently a series of isomorphous formates $(NH_4)[M^{II}(HCOO)_3]$ (M = Mn, Co, Ni) was reported[44] where anionic frameworks with the **acs** topology are composed of metals with octahedral coordination. At the same time, the overall arrangement of octahedral building blocks remains basically trigonal-prismatic. The space-group symmetry of the formates is $P6_322$, the site symmetry of building blocks is D_3, and every structure comprises a single (i.e., non-interpenetrated) anionic framework.

DUT-7(RT) has exactly the same space-group symmetry ($P6_322$) as the formates discussed above, but the site symmetry of the building blocks is only C_3 since in our case the point-group symmetry of an isolated SBU is T_d (it cannot possess D_3 symmetry upon any distortion because D_3 is not a subgroup of T_d. Such group-subgroup considerations hold for an ordered arrangement of SBUs.

(37) Kesanli, B.; Cui, Y.; Smith, M. R.; Bittner, E. W.; Brockrath, B. C.; Lin, W. *Angew. Chem., Int. Ed.* **2005**, *44*, 72–75.
(38) Yue, Q.; Sun, Q.; Cheng, A.-L.; Gao, E.-Q. *Cryst. Growth Des.* **2010**, *10*, 44–47.
(39) Ravon, U.; Domine, M. E.; Gaudillere, C.; Desmartin-Chomel, A.; Farrusseng, D. *New J. Chem.* **2008**, *32*, 937–940.
(40) Spek, A. L. *J. Appl. Crystallogr.* **2003**, *36*, 7–13.
(41) O'Keeffe, M.; Peskov, M. A.; Ramsden, S. J.; Yaghi, O. M. *Acc. Chem. Res.* **2008**, *41*, 1782–1789.
(42) Delgado Friedrichs, O.; O'Keeffe, M.; Yaghi, O. M. *Acta Crystallogr., Sect. A* **2003**, *A59*, 515–525.
(43) Sudik, A. C.; Cote, A. P.; Yaghi, O. M. *Inorg. Chem.* **2005**, *44*, 2998–3000.
(44) Wang, Z.; Zhang, B.; Inoue, K.; Fujiwara, H.; Otsuka, T.; Kobayashi, H.; Kurmoo, M. *Inorg. Chem.* **2007**, *46*, 437–445.

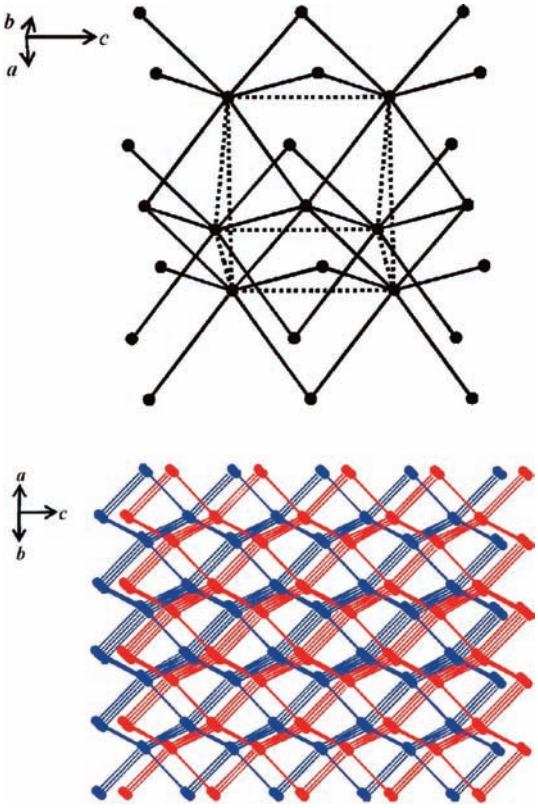

Figure 4. Top: Idealized **acs** net, the dotted lines represent the enclosed coordination polyhedron (trigonal prism); Bottom: Schematic view of the two interpenetrating networks within the structure of DUT-7.

If there is, for example, an orientational disorder in the crystal structure, then the averaged site symmetry of Zn_4O unit can be D_3 as it was indeed observed in MOF-177[45]). This lowering of the site symmetry and retaining the same space-group symmetry give rise to interpenetration. DUT-7 exhibits exactly two interpenetrated frameworks related by the 2-fold axes, the space-group symmetry of each individual framework is either $P6_3$ (DUT-7(RT)) or $P6_5$ (DUT-7(LT)). According to the classification of the interpenetration patterns proposed by Blatov et al., the structures belong to the interpenetration class IIa.[46] This is (to the best of our knowledge) the first occurrence of two interpenetrating **acs** nets. Up to now the only known examples of interpenetrated frames with **acs** topology have been isomorphous cyanometallates $Ln[Me(CN)_2]_3(H_2O)_3$ (Ln = Eu, Tb; Me = Au, Ag) consisting of three translationally equivalent frameworks each (interpenetration class Ia).[47] Concerning the "physical" reason for interpenetration in DUT-7(RT), one has to note that the distances between building blocks (controlled by the rather elongated linker) are large enough (18.27 Å) to "accommodate" an additional structure. For comparison, in the interpenetrated IRMOF-11 the distance between Zn_4O building blocks is 17.19 Å.[48]

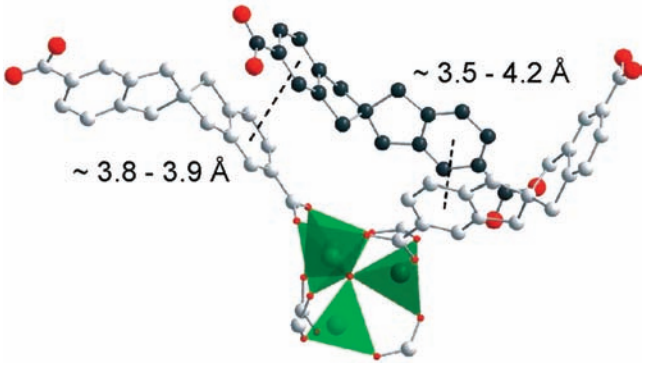

Figure 5. Linker shown in black is stacked with two linkers from the second interpenetrating network by $\pi-\pi$ interactions.

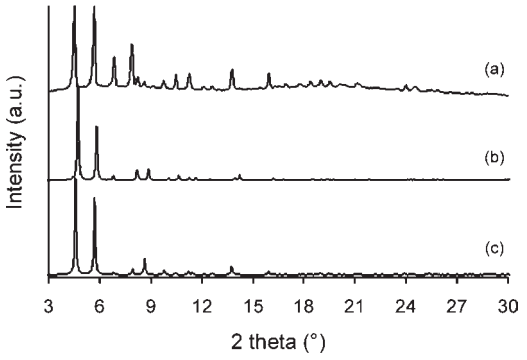

Figure 6. PXRD pattern of (a) the as-made MOF DUT-7. In comparison the calculated patterns for (b) DUT-7(LT) and (c) DUT-7(RT) are shown.

The crystal structure of DUT-7 and the formates discussed above present examples that the formation of a MOF, and its topology are predetermined not only by the geometry of the building blocks as is usually assumed[49] but are also linker-dependent.[50] In this respect, the recent synthesis of a MOF comprising Zn_4O building units connected by 5-methylisophthalate anions into a framework with quite rare **lcy** topology has to be mentioned.[51]

Further Characterization of DUT-7 and Synthesis of Zn_4O(*rac*-L)$_3$ (DUT-7(*rac*)). Since no solvent molecules could be localized within the crystal structure of DUT-7(RT), the molecular formula of this compound had to be determined by elemental analysis in combination with thermogravimetric analysis (Supporting Information, Figure S3). According to these results, DUT-7 contains 10 DMF molecules and 3.5 molecules of water per formula unit.

Though the crystal structure of DUT-7(RT) exhibits hexagonal channels filled with a large amount of solvent, it exhibits only a moderate porosity judging from the nitrogen physisorption measurement (Figure 7). According to this measurement the material exhibits a total pore volume of 0.13 $cm^3\ g^{-1}$ (p/p_0 = 0.99). Beside the low overall nitrogen uptake, the nitrogen physisorption isotherm shows a large hysteresis comparable to isotherms obtained for highly flexible polymers[52,53] or gate pressure

(45) Chae, H. K.; Siberio-Perez, D. Y.; Kim, J.; Go, Y. B.; Eddaoudi, M.; Matzger, A. J.; O'Keeffe, M.; Yaghi, O. M. *Nature* **2004**, *427*, 523–527.
(46) Blatov, V. A.; Carlucci, L.; Ciani, G.; Proserpio, D. M. *CrystEngComm* **2004**, *6*, 377–395.
(47) Baburin, I. A.; Blatov, V. A.; Carlucci, L.; Ciani, G.; Proserpio, D. M. *J. Solid State Chem.* **2005**, *178*, 2452–2474.
(48) Eddaoudi, M.; Kim, J.; Rosi, N.; Vodak, D.; Wachter, J.; O'Keeffe, M.; Yaghi, O. M. *Science* **2002**, *295*, 469–472.
(49) Ockwig, N. W.; Delgado-Friedrichs, O.; O'Keeffe, M.; Yaghi, O. M. *Acc. Chem. Res.* **2005**, *38*, 176–182.
(50) Furukawa, H.; Kim, J.; Ockwig, N. W.; O'Keeffe, M.; Yaghi, O. M. *J. Am. Chem. Soc.* **2008**, *130*, 11650–11661.
(51) Chun, H.; Jung, H. *Inorg. Chem.* **2009**, *48*, 417–419.
(52) Ghanem, B. S.; Msayib, K. J.; McKeown, N. B.; Harris, K. D. M.; Pan, Z.; Budd, P. M.; Butler, A.; Selbie, J.; Book, D.; Walton, A. *Chem. Commun.* **2007**, 67–69.

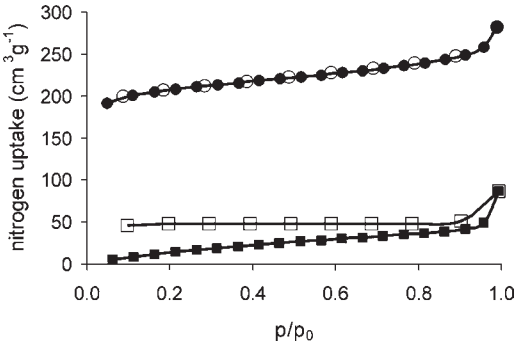

Figure 7. Nitrogen physisorption isotherm of DUT-7 (activated at 453 K, squares) and DUT-7(*rac*) (activated at 373 K, circles), closed symbols: adsorption, open symbols: respective desorption.

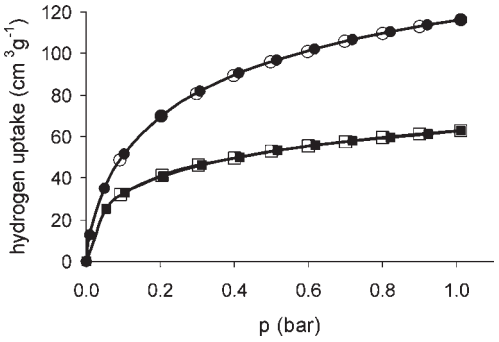

Figure 8. Hydrogen physisorption isotherm of DUT-7 (activated at 423 K, squares) and DUT-7(*rac*) (activated at 373 K, circles), closed symbols: adsorption, open symbols: respective desorption.

MOFs.[54] Because of that the specific surface area was determined from the desorption branch and amounts to 182 $m^2 g^{-1}$ (S_{BET}, p/p_0 = 0.1). In contrast to the result of the nitrogen physisorption measurement, the hydrogen uptake of DUT-7 at 77 K and 1 bar is surprisingly high (0.57 wt %, Figure 8). MOF-5 which exhibits a significantly higher specific surface area of 3,362 $m^2 g^{-1}$ shows a comparatively low hydrogen uptake of 1.32 wt % (1 bar, 77 K).[55] These findings support the assumption that the pore entrances of the evacuated framework are too small for the adsorption of nitrogen. On the contrary, the size of the pore openings could only be estimated from the crystal structure of the solvated compound. A further structural transformation occurs during activation (Supporting Information, Figure S1) because of the high degree of flexibility of the interpenetrated framework and leads to a loss of the crystallinity. The original structure of the framework could not be restored by resolvation with DMF.

Further attempts to obtain a porous MOF were carried out with the racemic mixture of the linker. The dicarboxylic acid *rac*-H_2L was heated with an excess of zinc nitrate in DMF to 393 K for 20 h leading to a microcrystalline solid DUT-7(*rac*) not containing any crystals suitable for single crystal X-ray analysis. According to the results obtained by elemental and thermogravimetric analysis of DUT-7(*rac*) (Supporting Information, Figure S4) the composition of the network is Zn_4O(*rac*-L)$_3$, too. In addition, 4 molecules of DMF and 2.3 molecules of water are included. The IR spectrum of the compound containing the racemic linker (Supporting Information, Figure S5) matches that of the material obtained with the enatiomeric pure linker. This finding is further support for the assumed framework composition of DUT-7(*rac*).

Though the framework compositions of DUT-7 and DUT-7(*rac*) are essentially the same, the PXRD pattern of both materials differ. In addition, the behavior during physisorption measurements varies. The nitrogen physisorption isotherm of DUT-7(*rac*) as it is shown in Figure 7 is typical for microporous materials (type I isotherm) whereas the nitrogen physisorption isotherm of DUT-7 showed a hysteresis. DUT-7(*rac*), desolvated at 373 K in vacuum, exhibits a total pore volume of 0.44 $cm^3 g^{-1}$ (p/p_0 = 0.99) and a specific surface area of 777 $m^2 g^{-1}$ (S_{BET}, p/p_0 = 0.1). The hydrogen physisorption measurement revealed a hydrogen storage capacity of 1.05 wt % H_2 at 77 K and 1 bar (Figure 8). After activation at 373 K, the PXRD pattern of DUT-7(*rac*) had changed significantly (Supporting Information, Figure S2). A change of the PXRD pattern is already observed for the material desolvated in vacuum at room temperature (Supporting Information, Figure S2). As it was found for DUT-7, the structure of DUT-7(*rac*) could also not be restored by resolvation with DMF.

The results of the PXRD and physisorption measurements after activation of the MOFs DUT-7 and DUT-7(*rac*) prove that both materials exhibit porosity and a high structural flexibility.

Conclusions

In summary, we have presented the successful integration of a chiral dicarboxylate comprising a spirobiindane backbone into a MOF, named DUT-7. For the first time, a three-dimensional porous framework built of a chiral spiro linker has been synthesized. The obtained material has an unprecedented crystal structure with a 2-fold interpenetrated framework significantly differing from that of the cubic IRMOF series though having the same framework composition. The crystal structure of DUT-7 undergoes a reversible structural transformation upon cooling, during which the former tetrahedral coordination of one zinc atom of the Zn_4O cluster is changed to an octahedral one caused by the additional coordination of two solvent molecules. This finding of cluster flexibility, without precedent up to now, could offer new insights into the catalytic activity of MOFs exhibiting only coordinatively saturated metal atoms such as MOF-5.

Acknowledgment. The authors thank the German Research Foundation within the priority program "Porous Metal-Organic Frameworks" (SPP 1362, MOFs) and the "Helmholtz-Zentrum Berlin für Materialien und Energie" for financial support, Dr. G. Auffermann (Max Planck Institute for Chemical Physics of Solids, Dresden) for the performance of the elemental analyses and Dr. R. Palkovits (Max Planck Institute for Coal Research, Mülheim) for the separation of enantiomers.

Supporting Information Available: Crystallographic data for compounds DUT-7(RT) and DUT-7(LT); additional PXRD patterns; TGA curves; and IR spectra. This material is available free of charge via the Internet at http://pubs.acs.org.

(53) Rose, M.; Boehlmann, W.; Sabo, M.; Kaskel, S. *Chem. Commun.* **2008**, 2462–2464.
(54) Fletcher, A. J.; Thomas, K. M.; Rosseinsky, M. J. *J. Solid State Chem.* **2005**, *178*, 2491–2510.
(55) Rowsell, J. L. C.; Millward, A. R.; Park, K. S.; Yaghi, O. M. *J. Am. Chem. Soc.* **2004**, *126*, 5666–5667.